Study of $\Upsilon(nS)$, J/ψ and $\psi(2S)$ production in PbPb collisions at LHCb

Author: Salma Zian Jamoldinova, szianjam53@alumnes.ub.edu Facultat de Física, Universitat de Barcelona, Diagonal 645, 08028 Barcelona, Spain.

Advisor: Ricardo Vázquez, rvazquez@ub.edu

Abstract: The production of $\Upsilon(nS)$ (n=1,2,3), J/ψ , and $\psi(2S)$ mesons has been studied in lead-lead collisions at the LHCb. In the search for Quark-Gluon Plasma, which suppresses more considerably excited states, the yield ratio between $q\bar{q}(2S)$ and $q\bar{q}(1S)$ (q=b,c) has been computed. The dimuon decay channel is considered to reconstruct the invariant mass of the quarkonia states, and unbinned maximum-likelihood fits are used to extract the yields. For $\Upsilon(nS)$, we find insufficient evidence for the production of $\Upsilon(2S)$, leading to an upper bound on the excited-to-ground state ratio of 0.09, significantly lower than the corresponding proton-proton collision value of 0.25 \pm 0.01, suggesting suppression. For charmonium, we distinguish between prompt and non-prompt production using the pseudo decay time and report a $\psi(2S)$ -to- J/ψ yield ratio of 0.022 \pm 0.004, which remains inconclusive but compatible with previous results from pp collisions.

Keywords: Heavy-ion collision, QGP, bottomonium, charmonium.

SDGs: Quality education, industry, innovation and infrastructure, and partnership for goals.

I. INTRODUCTION

Collisions of heavy ultra-relativistic nuclei are being studied as a way to better understand the Quark-Gluon Plasma (QGP), a state of deconfined quarks and gluons that filled the early stages of the universe. More specifically, the suppression of quarkonia, bounded states of a heavy quark and antiquark, and its impact on the excited and ground states is one of the ways we have to determine the formation of QGP [1].

At high temperatures and energy densities, QGP formation and the corresponding suppression of the heavy quark potential due to the color screening [1] in the plasma, causes the deconfinement of $q\bar{q}$ pairs, leading to the suppression mentioned above. Calculations using lattice quantum chromodynamics (QCD) predict that it affects excited states more than those with a higher binding energy. At the same time, heavier quarks like charm and beauty are generally produced at the beginning of the collision, therefore experiencing the entire QGP evolution [2].

When considering the suppression of J/ψ and its excited states, one finds that it is smaller than initially expected considering QGP. To understand this, we must account for the uncorrelated (re)combination of $c\bar{c}$ to form charmonium states. This phenomenon increases with the number of heavy quarks produced in the collision [3]; as such, the recombination is higher in J/ψ production compared to Υ production since there are fewer $b\bar{b}$ pairs produced in one collision than $c\bar{c}$. Considering this, makes us question whether there is a higher suppression ratio of states with lower binding energies relative to ground states in $\Upsilon(nS)$, a $b\bar{b}$ meson, than in J/ψ , a $c\bar{c}$ meson.

It is essential to mention that the suppression observed in the production of the excited states of these mesons cannot be exclusively associated with the presence of QGP, as other competing effects, such as cold nuclear matter (CNM) effects [4], may also play a role. Finally, while discussing J/ψ , we need to distinguish between prompt and non-prompt production [5]. Prompt production considers the particles directly produced at the collisions. In contrast, non-prompt has a production vertex displaced from the primary vertex since it originates from decays of bottom hadrons. It is significant to notice this since the processes given by the presence of QGP, like suppression or recombination, mainly affect prompt production.

In this work, we study the production of J/ψ , $\psi(2S)$, and $\Upsilon(nS)$ in PbPb collisions through the dimuon decay channel. First, we define several variables, which afterward are considered to filter the data. With this, we use the unbinned maximum likelihood method to fit the data, and then we compute the ratio of excited states to ground state. This rate is then compared to pp collisions to determine whether there is suppression and then pinpoint if it is more notorious in the bottomonium than in the charmonium states, as expected.

II. DATA ANALYSIS

A. Particle detection

The data used throughout the project comes from the LHCb detector [6]. The LHCb experiment is a single-arm forward spectrometer that studies particles containing beauty and charm quarks. Its tracking system can measure the momentum of charged particles. A calorimetric system is employed to identify photons, electrons, and hadrons. Muons are identified by a system of alternating layers of iron and a multi-wire proportional chamber.

To study the production of Υ and J/ψ , we use the μ^+ μ^- decay mode:

$$\Upsilon(nS) \to \mu^+ \mu^-, \quad \text{and} \quad J/\psi \to \mu^+ \mu^-.$$
 (1)

We then compute its invariant mass given the energy and the momentum of the muons:

$$M_{\mu^{+}\mu^{-}} = \sqrt{(E_{\mu^{+}} + E_{\mu^{-}})^{2} - (p_{\mu^{+}} + p_{\mu^{-}})^{2}}.$$
 (2)

Plotting this mass, we observe whether peaks appear at the tabulated masses of the searched particles.

B. Event selection

The data is filtered via an offline selection. When considering the muons used to select the candidates, a good track-fit quality and vertex reconstruction fit are required. Particle identification (PID) criteria are applied to suppress the background from random combinations of tracks. The transverse momentum for the dimuon candidates of J/ψ has to satisfy $p_{\rm T} > 750$ MeV, and for Υ , $p_{\rm T} > 1$ GeV.

Finally, to distinguish the prompt from non-prompt production of J/ψ , the distribution of the pseudo decay time t_z is used, which is defined as:

$$t_z = \frac{(z - z_{PV}) \cdot m}{p_z},\tag{3}$$

where z is the decay vertex z coordinate of the J/ψ candidate, z_{PV} is the production vertex z coordinate, m is the known invariant mass, as provided by the Particle Data Group (PDG) [7], and p_z is the momentum in the z coordinate.

C. Fit

When considering the yields of the particles and their corresponding fits, one has to talk about Gaussian distributions and Crystal Ball (CB) functions.

The Gaussian distribution is given by:

$$f(x; \mu, \sigma) = \frac{1}{\sqrt{2\pi\sigma^2}} \cdot \exp\left(-\frac{(x-\mu)^2}{2\sigma^2}\right),$$
 (4)

where μ is the mean and σ is the standard deviation.

The Crystal Ball function is a normal distribution with a tail that follows a power law below a certain threshold. It has the same parameters as the Gaussian distribution and two additional ones:

$$f(x; \mu, \sigma, n, \alpha) = N \begin{cases} \exp\left(-\frac{(x-\mu)^2}{2\sigma^2}\right) & \text{if } \frac{(x-\mu)}{\sigma} > -\alpha \\ A \cdot \left(B - \frac{x-\mu}{\sigma}\right)^{-n} & \text{if } \frac{(x-\mu)}{\sigma} \le -\alpha, \end{cases}$$
(5)

where n is the power at which the tail decays and α is the threshold at which it begins to decay in terms of the standard deviation. This second distribution is observed when sufficient data is available, as charged particles lose energy and alter their linear momentum when accelerating due to Bremsstrahlung radiation, leading to a shift in the detected invariant mass.

For $\Upsilon(1S)$ and its excited states, the signal is modeled by a Gaussian distribution, while for J/ψ and $\psi(2S)$, Crystal Ball functions are used. In both cases, the separation between the two peaks representing the 1S and 2S states is fixed to the known difference in invariant mass for the two states, as reported by the PDG [7]. The σ , n, and α of the second peak are fixed to those of the ground state peak, as they are determined by the detector's resolution. This resolution, in turn, depends on the linear momentum, which is, on average, practically the same for particles with comparable invariant masses. Chebyshev polynomials are used to describe the background.

Lastly, unbinned maximum-likelihood fits are employed to determine the model's free parameters, such as the mean or standard deviation of the first peak. Given a sample of data points and a specific distribution used to model them, the likelihood function quantifies how likely it is to observe the data under the given distribution. This function depends on the parameters of the distribution. By maximizing the likelihood function, one determines the parameter values that make the observed data most probable. The term "unbinned" indicates that individual data points are considered directly, and the choice of binning does not influence the resulting parameter estimates.

III. RESULTS

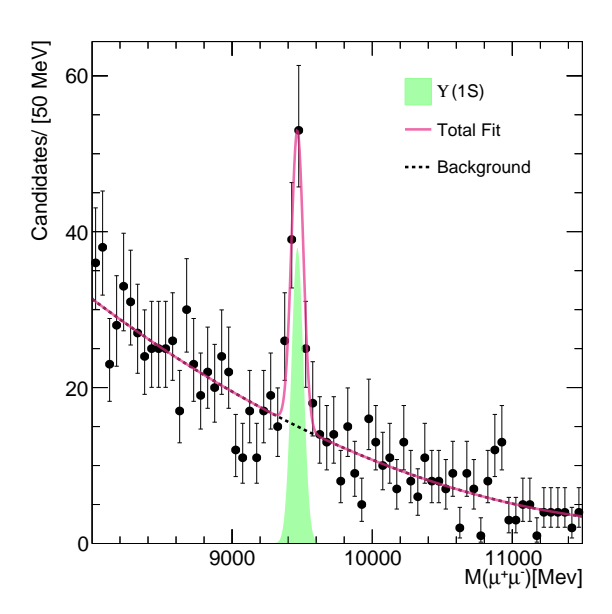
A. $\Upsilon(nS)$ production

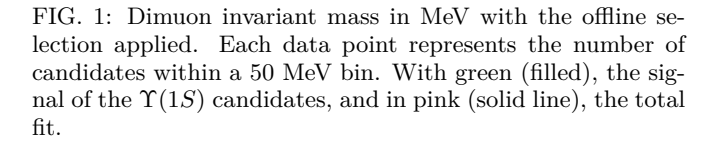
Representing the filtered data of the dimuon invariant mass within the range of the $b\bar{b}$ bound states, and performing an unbinned maximum likelihood fit using a normal distribution for the most prominent peak, corresponding to $\Upsilon(1S)$, yields figure (1). Nevertheless, in light of the possibility of an excited state, $\Upsilon(2S)$, a second Gaussian distribution is fitted, as described in the fitting subsection. This results in (2). No $\Upsilon(3S)$ is detected, and since the signal for $\Upsilon(2S)$ is already weak, no signal component accounting for the $\Upsilon(3S)$ is added into the fit.

The yield for $\Upsilon(1S)$ is 81 ± 14 for the first fit and 81 ± 16 for the second. For $\Upsilon(2S)$, the yield is 7 ± 6 . The signal corresponding to the second peak is barely discernible, consistent with the absence of excited states.

Adding new parameters to a fit increases the likelihood that the considered model describes better the given dataset, as evidenced by comparing the unbinned maximum likelihood values for the two fits. However, it is crucial to determine whether the improvement is substantial enough to justify the additional parameters. To evaluate this, we employ the likelihood ratio test (LRT) [8].

The likelihood ratio test is a hypothesis test used to compare the goodness of fit between two competing statistical models. These models must be nested, meaning that one can be reduced into the other by imposing con-





straints on its parameters. In this work, the two fits differ by a single parameter: the amplitude of the second peak. By setting this amplitude to zero, the two-peak fit simplifies to the one-peak fit.

We begin defining the null hypothesis as the more constrained model, which assumes the presence of only one peak, corresponding to $\Upsilon(1S)$. On the other hand, the alternative hypothesis posits the presence of two peaks representing both the ground state and the excited state. The likelihood ratio is given by:

$$\lambda_{\rm LR} = -2 \cdot \ln \left(\frac{\mathcal{L}_1^{\rm max}}{\mathcal{L}_2^{\rm max}} \right),$$
 (6)

where \mathcal{L}_1^{\max} and \mathcal{L}_2^{\max} represent the maximum likelihoods of the null and alternative hypotheses, respectively. If the null hypothesis is correct, λ_{LR} asymptotically follows a χ^2 distribution. Furthermore, when the two models differ by a single parameter, the square root of λ_{LR} corresponds to the number of standard deviations between the two fits. If the significance is below 3σ , the null hypothesis is strongly supported. Conversely, if it exceeds 3σ , the evidence favors the two-peak model, indicating the presence of excited states. Finally, if the significance surpasses 5σ , the null hypothesis is rejected, and the two-peak model is deemed correct.

For our two models, we obtain a standard deviation of 1.2σ . As a result, we conclude that the null hypothesis is valid: the additional parameter in the distribution is unjustified

In light of these results, we cannot provide conclusive

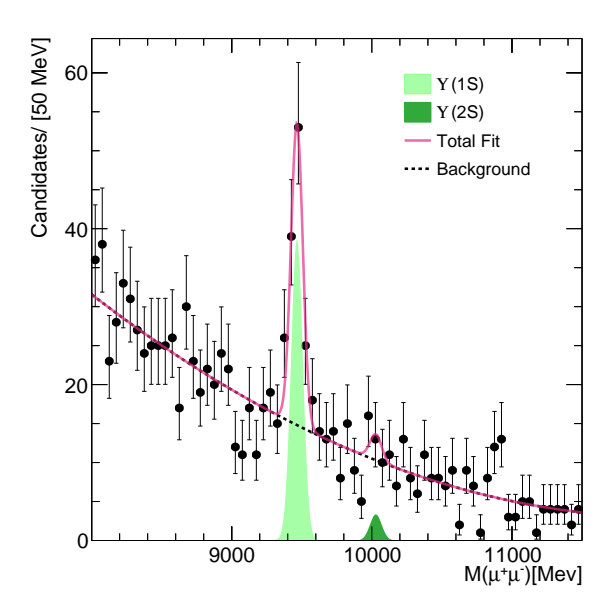


FIG. 2: Dimuon invariant mass in MeV with the offline selection applied. Each data point represents the number of candidates within a 50 MeV bin. With light green (filled), the signal of the $\Upsilon(1S)$, with darker green (filled) the signal of the $\Upsilon(2S)$ candidates, and in pink (solid line), the total fit.

values for the production rate of the excited state versus the ground state, as there is insufficient evidence to support the production of $\Upsilon(2S)$. However, we can establish an upper bound for this rate. Considering the yields of the two-peak model, we obtain an upper-bound rate of 0.09. The value reported by LHCb for proton-proton collisions is 0.25 ± 0.01 [9]. These two rates differ by more than 5 times the reported uncertainty, indicating a suppression of the less bounded state, $\Upsilon(2S)$, compared to the ground state. Our value can also be compared to results from proton-lead collisions in which the obtained ratio is 0.22 ± 0.02 [10]. This result is also incompatible with our rate, further confirming the increased suppression of the excited state.

This suppression is also consistent with the findings of the ALICE [11] and ATLAS [2] collaborations, in which they obtained a decrease in the signal when comparing less bounded states to the ground state.

Finally, no $\Upsilon(3S)$ is detected, which further indicates the suppression of excited states compared to the ground state, more so considering that the 3S state is even less energetically bounded than the 2S.

The results found in this work should, however, not be interpreted as unequivocal proof of the presence of QGP, as there may be competing mechanisms, such as the CNM effect, which were not accounted for. Nevertheless, the observed suppression in the excited state highlights the importance of conducting further experiments with larger datasets to study this phenomenon in greater detail.

B. J/ψ and $\psi(2S)$ production

When analyzing the production of $c\bar{c}$ bound states after filtering raw data, it is crucial to differentiate between particles produced directly at the collision and those originating from the decay of heavier particles, particularly in studies aiming to identify suppression in excited states as potential evidence of QGP. Non-prompt production occurs away from the collision point, thus outside the region where the QGP forms. As such, suppression and recombination caused by the presence of QGP are expected to predominantly impact prompt-produced mesons.

This distinction can be achieved using the pseudo decay time, as defined in equation 3. Particles produced via prompt production are generated instantaneously during the collision and decay shortly thereafter. As a result, their pseudo decay time distribution is a delta function centered at $t_z=0$. However, due to the finite resolution of the detector, this delta function must be convolved with the resolution function, typically modeled by a two-Gaussian distribution. The outcome of this convolution is a single normal distribution centered at zero.

Conversely, particles produced via non-prompt production, originating from the decay of b-hadrons, have significantly longer pseudo decay lifetimes due to the non-negligible lifetime of the b-hadrons. Their t_z distribution follows an exponential decay law, allowing for their distinction. As the pseudo decay time for non-prompt production is substantially longer, the resolution function of the detector is generally not considered in this case.

To plot the t_z distribution, first, we consider the totality of the data after the offline selection without separating prompt from non-prompt production, and then we make an unbinned maximum likelihood fit of the dimuon invariant mass with two CB functions for the J/ψ and $\psi(2S)$ peaks. With the obtained values of the fit, we plot the t_z distribution of all the candidates within 2σ of the obtained mean for the J/ψ mass. Using this data, we perform an unbinned maximum likelihood fit of the t_z distribution using a Gaussian distribution for the peak. From this, we get figure 3.

It is seen that, in addition to the normal distribution centered at $t_z=0$ ps, there is a non-zero component on both sides, which is asymmetrical. On the left side (negative values), the contribution is primarily due to the background of the signal. However, on the right side (positive values), there are two contributions to consider: the background, as observed on the left, and the non-prompt production of J/ψ candidates. If there were no non-prompt production, the distribution would be symmetric. It is important to note that both contributions (background and non-prompt production) follow an exponential law.

We can also observe from the plot, that the prompt contribution, represented by the pink distribution, is approximately confined within $t_z = -0.1$ ps and $t_z = 0.1$ ps. Based on this observation, we adopt a reasonable approximation: prompt-produced particles will be defined

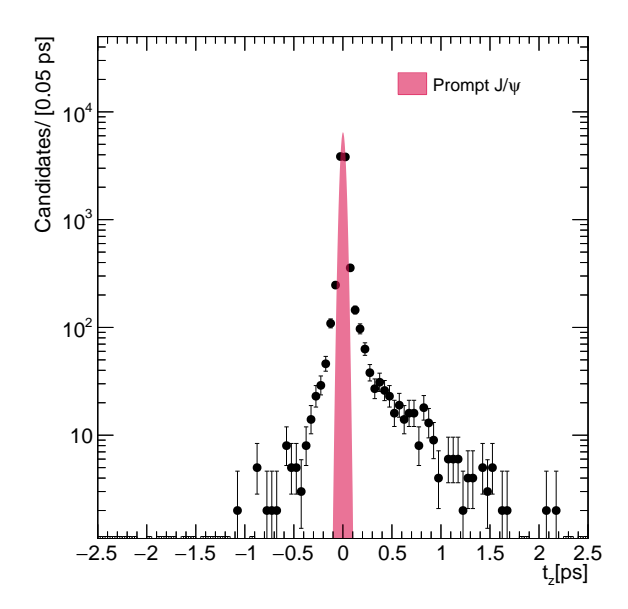


FIG. 3: Pseudo decay time distribution for the J/ψ candidates. Each data point represents the number of candidates within a 0.05 ps bin. In pink (filled), the contribution of prompt production in the distribution.

as those with a pseudo decay time shorter than 5σ , where σ is the standard deviation of the fitted distribution, thus resulting in $|t_z| < 0.125$ ps. Under this assumption, we can now examine the invariant mass for the reconstructed dimuons in the expected range for $c\bar{c}$ mesons. The resulting plot is shown in figure 4. In this case, the yield for the prompt produced J/ψ is $(7.97 \pm 0.15) \cdot 10^3$, and for $\psi(2S)$ it is 172 ± 30 . For $c\bar{c}$ mesons, we can confidently affirm that excited states are detected.

Using these yields, we compute the ratio of $\psi(2S)$ -to- J/ψ , obtaining 0.022 ± 0.004 . Since the data for prompt production signal in proton-proton collisions [5] at LHCb is not explicitly available, we instead obtain the signal ratio as:

$$\frac{\sigma_{\psi(2S)}}{\sigma_{J/\psi}} \times \frac{\mathcal{B}_{\psi(2S)\to e^+e^-}}{\mathcal{B}_{J/\psi\to\mu^+\mu^-}} = \frac{N_{\psi(2S)}}{N_{J/\psi}} \times \frac{\epsilon_{\text{tot},J/\psi}}{\epsilon_{\text{tot},\psi(2S)}}, \quad (7)$$

where the first term is the ratio of cross-sections, the second the ratio of branching fractions, the third the yield ratio, and the fourth the efficiency ratio. This approach accounts for the relative efficiencies between $\psi(2S)$ and J/ψ , which are not considered in this work. Nonetheless, assuming that the efficiencies for the excited and ground states are approximately equal (i.e., the ratio is close to 1) due to the similar magnitudes of energy and momentum, this serves as a reasonable first-order approximation.

The value provided by the LHCb collaboration is 0.0196 ± 0.0004 [5]. Since these two values are compatible, we could suggest that the increased suppression of the excited state is less noticeable when considering $\psi(2S)$ because of the effects of recombination. However, due to the

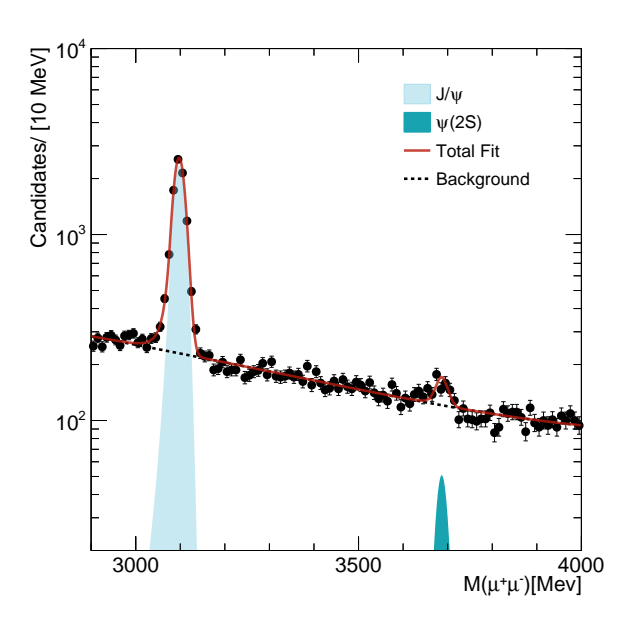


FIG. 4: Dimuon invariant mass in MeV with the offline selection applied. Each data point represents the number of candidates within a 10 MeV bin. With light blue (filled), the signal of the J/ψ , with darker blue (filled) the signal of the $\psi(2S)$ candidates, and in red (solid line), the total fit.

significant approximations made when comparing these two values, the outcome remains inconclusive. Nevertheless, considering the available literature and the results reported by other LHC collaborations, such as CMS [3], which indicate an increased suppression of excited states, we reject the initial idea of an increased ratio due to recombination.

IV. CONCLUSIONS

The suppression of excited states relative to the ground state of bottomonium and charmonium is studied in this work. Enhanced suppression of $\Upsilon(2S)$ is observed, supporting the necessity for additional data to further investigate this phenomenon in the context of QGP formation. For $c\bar{c}$ states, the results remain inconclusive.

To improve the study, we should address several adjustments. First, the ratio of cross-sections should be computed instead of the yield ratio, as the latter does not account for efficiencies. Moreover, the cross-section ratio allows for direct comparison with theoretical predictions. Additionally, we would have to consider competing effects to determine whether the suppression is solely a consequence of QGP presence or whether other factors, like CNM, are involved. Finally, when considering the pseudo decay time for prompt production, we should use the Gaussian distribution resulting from the convolution of the detector resolution function and the delta distribution of the prompt-produced particles rather than simply applying a cut at $|t_z| < 0.125$ ps.

Acknowledgments

I would like to express my gratitude to my advisor, Dr. Ricardo Vázquez, for his invaluable help and guidance throughout this work. His patience and encouragement have had a truly significant impact. I would also like to thank my family and friends for their insights during this project—not only for their support but also for their care and encouragement over the years.

^[1] Matsui, T., & Satz, H. (1986). J/ψ suppression by quark-gluon plasma formation. *Physics Letters B*, 178(4), 416-422. https://doi.org/10.1016/0370-2693(86)91404-8.

^[2] ATLAS Collaboration. (2023). Production of $\Upsilon(nS)$ mesons in Pb+Pb and pp collisions at 5.02 TeV. Physical Review C, 107(5), 054912. https://doi.org/10.1103/PhysRevC.107.054912.

^[3] CMS Collaboration. (2017).Relative Modification of Prompt $\psi(2s)$ and J/ψ Yields from pp to PbPb Collisions at $\sqrt{s_{NN}}$ 5.02 TeV. *Physical* ReviewLetters, 118(16), 162301. https://doi.org/10.1103/PhysRevLett.118.162301.

^[4] LHCb Collaboration. (2024). Measurement of the $\psi(2S)$ to J/ψ cross-section ratio as a function of centrality in PbPb collisions at $\sqrt{s_{NN}}=5.02$ TeV. arXiv preprint, arXiv:2411.05669 (2024). https://arxiv.org/abs/2411.05669.

^[5] LHCb Collaboration (2024). Multiplicity dependence of $\sigma_{\psi(2S)}/\sigma_{J/\psi}$ in pp collisions at $\sqrt{s}=13$ TeV. Journal of High Energy Physics, 2024(5), 243. https://doi.org/10.1007/JHEP05(2024)243.

^[6] LHCb Collaboration. (2008). The LHCb detector at the LHC. Journal of Instrumentation, 3(08), S08005. https://doi.org/10.1088/1748-0221/3/08/S08005.

^[7] Particle Data Group. "The Review of Particle Physics." PDG. https://pdg.lbl.gov/.

^[8] Casella, G., & Berger, R. L. (2001). Statistical Inference (2nd ed.). Duxbury Press. ISBN 0-534-24312-6.

^[9] The LHCb Collaboration. (2023). Measurement of Υ production in pp collisions at $\sqrt{s_{NN}}=5$ TeV. Journal of High Energy Physics, 2023(7), 69. https://doi.org/10.1007/JHEP07(2023)069.

^[10] LHCb Collaboration. (2018). Study of Υ production in pPb collisions at $\sqrt{s_{NN}}=8.16$ TeV. Journal of High Energy Physics, 2018(11), 194. https://doi.org/10.1007/JHEP11(2018)194.

^[11] ALICE Collaboration (2021). Υ production and nuclear modification at forward rapidity in Pb–Pb collisions at $\sqrt{s_{NN}} = 5.02$ TeV. *Physics Letters B, 822,* 136579. https://doi.org/10.1016/j.physletb.2021.136579.

Estudi de la producció d' $\Upsilon(nS)$, J/ψ i $\psi(2S)$ en col·lisions PbPb al LHCb

Author: Salma Zian Jamoldinova, szianjam53@alumnes.ub.edu Facultat de Física, Universitat de Barcelona, Diagonal 645, 08028 Barcelona, Spain.

Advisor: Ricardo Vázquez, rvazquez@ub.edu

Resum: S'ha estudiat la producció dels mesons $\Upsilon(nS)$ $(n=1,2,3),\ J/\psi$ i $\psi(2S)$ en col·lisions plom-plom al LHCb. En cerca del Quark-Gluon Plasma, que suprimeix més considerablement els estats excitats, s'ha calculat el quocient entre el senyal de $q\bar{q}(2S)$ i $q\bar{q}(1S)$ (q=b,c). Per reconstruir la massa invariant dels estats de quarkonia, s'ha utilitzat el canal dimuònic de desintegració i s'han fet ajustos de màxima versemblança per obtenir els senyals. Per $\Upsilon(nS)$, no s'obté prou evidència que confirmi la producció d' $\Upsilon(2S)$, així doncs, es calcula una cota superior d'aquest quocient de 0.09, considerablement inferior als valors corresponents a les col·lisions protó-protó de 0.25 ± 0.01 , cosa que suggereix supressió. Pel charmonium, diferenciem entre la producció "prompt" i "non-prompt" mitjançant el pseudo temps de desintegració i reportem una quocient de 0.022 ± 0.004 , que és poc concloent però compatible amb resultats previs de les col·lisions pp.

Paraules clau: Col·lisió d'ions pesants, QGP, bottomonium, charmonium.

ODSs: Aquest TFG està relacionat amb els Objectius de Desenvolupament Sostenible (SDGs)

Objectius de Desenvolupament Sostenible (ODSs o SDGs)

1. Fi de la es desigualtats		10. Reducció de les desigualtats	
2. Fam zero		11. Ciutats i comunitats sostenibles	
3. Salut i benestar		12. Consum i producció responsables	
4. Educació de qualitat	Х	13. Acció climàtica	
5. Igualtat de gènere		14. Vida submarina	
6. Aigua neta i sanejament		15. Vida terrestre	
7. Energia neta i sostenible		16. Pau, justícia i institucions sòlides	
8. Treball digne i creixement econòmic		17. Aliança pels objectius	X
9. Indústria, innovació, infraestructures	Х		